International Journal of Progressive Sciences and Technologies (IJPSAT)
ISSN: 2509-0119.

https://ijpsat.org/
Vol. 53 No. 2 November 2025, pp. 396-414

Dimensioning And Design Of A Dry Distillation Prototype - Process Optimization

[1]Frank Marius RANDRIAMBAO, [2]Achille RAVONINJATOVO, [3]Lala ANDRIANAIVO.

[1] Ecole Normale Supérieure pour l'Enseignement Technique, ENSET
Université Antsiranana, BP 0
Antsiranana 201, Madagascar
Email : randfrmarius@yahoo.fr
[2] Centre National de Recherches Industrielle et Technologique, BP 6294 Fiadanana Antananarivo, Madagascar.
Email : Cnrit @moov.mg
[3] Ecole Supérieure Polytechnique, ESPA
Université d'Antananarivo, BP 1500
Antananarivo 101, Madagascar
Corresponding Author: Frank Marius RANDRIAMBAO. E-mail: randfrmarius@yahoo.fr

Abstract: This article focuses on the dimensioning and design of a dry-run distillation prototype - process optimization. First of all, the aim is to determine the dimensions of the crucible and the distiller by calculation. The method used is elementary cylinder geometry. Then, in the second part, we modeled the distiller temperature using two solution methods: the solve a one-dimensional heat equation with its imposed limit of conditions in temperature and heat flux, and the approximate Galerkin finite element method to obtain the actual and approximate profiles of the radial temperature field. Finally, we optimized the yield of the reaction taking place in the distillation crucible. The method used is response surface modeling. The model obtained is a 2nd degree linear equation with six parameters. The model coefficients are estimated using the multiple linear regression method. The results obtained using the methods adopted correspond, on the one hand, to the dimensions calculated by other authors, and the distiller temperature profiles (exact and approximate) simulated by Matlab are similar to each other up to 360°C. Thus, the difference between the simulated maximum temperature of the distiller and that measured in its crucible is around 74.4°C. This is due to the temperature gradient in the thickness of the refractory brick, which acts as thermal insulation for the distiller. On the other hand, the yields calculated from the products recovered during the 18 experimental tests on used tires (light vehicle LV, bicycle BL, and motorcycle MT) are consistent with the optimal yields estimated by the model.

Key-words: Dimensions, Crucible, Distiller, Temperature, Galerkin, Yield, Reaction, Model.

1. INTRODUCTION

The dimensioning and design of a dry distillation prototype requires detailed study while reducing its volume to achieve better efficiency.

Closed distillers are widely used in the chemical, petrochemical, and biochemical industries for the production of products of various qualities. The process involved are discontinuous and versatile. They have limited production volume and complex and sometimes unpredictable reaction systems [1].

International Journal of Progressive Sciences and Technologies (IJPSAT)
ISSN: 2509-0119.

https://ijpsat.org/
Vol. 53 No. 2 November 2025, pp. 396-414

For dry-run distillers, rubber materials (tires) can be introduced into the distiller in a single batch and emptied, also in a single batch, at the end of the process. The system remains closed during the process, meaning that there is no material gain. This method is also known as the static method [2].

This type of distiller is the simple that can be used for chemical transformation. It consist of a container into which the rubber is introduced at the beginning of the process; After setting the temperature and pressure conditions, the transformation continues until the desired conversion rate is achieved.

To design the best distiller for a given reaction, it is first necessary to choose the factors that are most important, which may be [3]:

- The conversion rate of a given reactant;

- The yield of the desired product;

- Minimization of the formation of impurities that are very difficult to separate or likely to cause problems (for safety, the environment, destruction, etc.);

- Minimization of the over all volume, in other words, maximization of production capacity or minimization of investment;

- The quality of the product obtained.

This article focuses on the dimensioning and design of a dry-run distiller prototype. The first part of this article is theoretical, consisting of sizing the prototype and determining the distiller temperature profile and the optimal reaction yield. The second part is devoted to the construction of the prototype and the simulation of the temperature profile and optimal yield.

2. MATERIALS AND METHODS

2.1 Materials

SolidWorks software is used to graphically represent the dry distillation prototype.

Matlab software is used to represent the temperature profile and the optimal yield profile.

The precision mechanical workshop is used to design the prototype.

2.2 Methods

In this section, we dimension the prototype according to the basic geometry of the cylinder. We determine the temperature profile of the distiller using the finite element method (FEM) and the optimal yield using the response surface method (RSM).

2.2.1 Crucible dimensions

The volume of gas in the distiller corresponds to the total volume of the distiller minus the volume of the tire bed (crucible).

The tire bed is composed of steel and pyrolyzable material; it's a material that will produce carbon black or solid residues, light gas, and heavy gas condensable into oil. When the bed reacts, the solid residues produced remain in the bed, so its mass is only reduced by the production of heavy and light gases. It is assumed that the average density of the bed remains roughly the same. By performing a mass balance on the tire bed under variable conditions, we can write [4]:

$$\rho_{tire} \frac{dV_{tire}}{dt} = -\omega_{hc} \quad (1)$$

Where ω_{hc} is the flow rate of heavy and light hydrocarbons produced by pyrolysis of the tire bed [kg/h].

V_{tire} : tire volume (m^3).

International Journal of Progressive Sciences and Technologies (IJPSAT)
ISSN: 2509-0119.

https://ijpsat.org/
Vol. 53 No. 2 November 2025, pp. 396-414

ρ_{tire} : tire density (kg/m^3).

Or $Q_v = \frac{\omega_{hc}}{\rho_{tire}}$ (2)

Equation (1) becomes:

$$\frac{dV_{tire}}{dt} = -Q_v \quad (3)$$

Where Q_v : gas volume flow (m^3/h).

The gas volume flow rate is calculated by equation 4:

$$Q_V = \pi R_{crucible}^2 v_z \quad (4)$$

Where $R_{crucible}$: crucible radius (m).

v_z : gas surface velocity (m/s).

First, we choose a surface velocity for the circulation of the heat transfer fluid (gas) in the crucible, v_z, which for the gas volume flow Q_{gas} to be satisfied, conditions the value of the crucible's cross-sectional area, and therefore its diameter $D_{crucible}$.

For a gas, v_z satisfies $0,1 \langle v_z \langle 10 m/s$.

We take $v_z \approx 5 m/s$.

If we take the cylindrical radius of the crucible $R_{crucible}$ of the thermogravimetric instrumented research pilot (PRITherm) equal to 45mm [5], we obtain:

$Q_V = 0,03 m^3/s$.

It's important to bear in mind that as the process proceeds, the volume of the tire bed is reduced. The gas volume increases as the bed volume decreases. This gives:

$$\frac{dV}{dt} = -\frac{dV_{tire}}{dt} = Q_v \quad (5)$$

Where V : gas volume (m^3).

The crucible has the shape of a cylinder with internal radius $R_{crucible}$ and height $H_{crucible}$. Its volume can be determined as follows [6]:

$$V_{crucible} = \pi R_{crucible}^2 H_{crucible} \quad (6)$$

Where $V_{crucible}$: crucible volume (L).

International Journal of Progressive Sciences and Technologies (IJPSAT)
ISSN: 2509-0119.

https://ijpsat.org/
Vol. 53 No. 2 November 2025, pp. 396-414

$H_{crucible}$: crucible height (mm).

Fig.1 shows the distillation crucible.

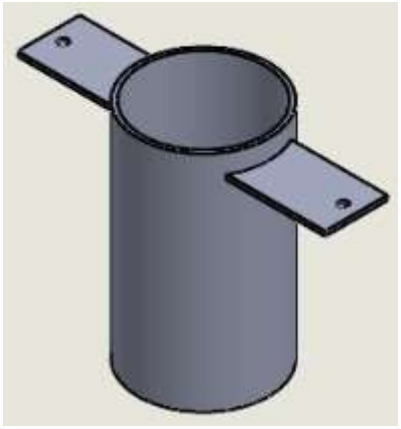

Figure1: *Distillation crucible [7].*

The height of the crucible can be determined by calculating the volume of the crucible from the inequality ratio as follows: $1 \leq \frac{H_{crucible}}{D_{crucible}} \leq 20$ [8].

Hence $D_{crucible} \leq H_{crucible} \leq 20D_{crucible}$, or $90mm \leq H_{crucible} \leq 1800mm$.

We deduce the crucible volume:

$$0,57L \leq V_{crucible} \leq 11,45L \quad (7)$$

2.2.2 Distiller dimensions

Having obtained an order of magnitude for the volume of the crucible placed in the distillator, we can be deduced the volume of the distillator $V_{distillator}$.

The dimensions of the distillator (assumed to be cylindrical) can be determined on the basis of the volume $V_{distillator}$: its height $H_{distillator}$, its diameter $D_{distillator}$, respecting the inequality ratio, which ensures that the distillator's height is greater than its diameter.

The volume of the distiller is given by the following formula [6]:

$$V_{distillator} = \pi R^2_{distillator} H_{distillator} \quad (8)$$

Where $V_{distillator}$: distiller volume (L).

$R_{distillator}$: distiller radius (mm).

$H_{distillator}$: distiller height (mm).

We choose a distillator radius greater than that of the crucible, so the height $H_{distillator}$.

International Journal of Progressive Sciences and Technologies (IJPSAT)
ISSN: 2509-0119.

https://ijpsat.org/
Vol. 53 No. 2 November 2025, pp. 396-414

For a distillator radius $R_{distillator}$=150mm and a distillator height $H_{distillator}$=330mm, the volume becomes:

$$V_{distillator} = 23L.$$

The distiller diameter can be chosen to be greater than the crucible diameter, or calculated using the following formula [6]:

$$D_{distillator} = 2 \times R_{distillator} \quad (9)$$

Or $D_{distillator} = 330mm$.

The ratio $\frac{H_{distillator}}{D_{distillator}} \geq 1$ is verified.

Fig.2 shows the distiller.

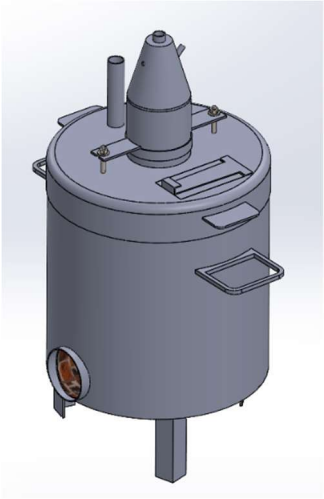

Figure 2: *Distiller [7].*

Thickness is calculated according to API (American Petroleum Institute) standard 650 [9]

$$e_{distillator} = \frac{4,9 D_{distillator} \left(H_{distillator} - 0,3 \right) G}{S_d} + CA \quad (10)$$

With $e_{distillator}$: Distiller thickness (mm).

S_d : permissible limits of materials used.

$D_{distillator}$: Distiller diameter.

$H_{distillator}$: Height of distiller.

G: density of reagent used (for liquid, G=0,98).

International Journal of Progressive Sciences and Technologies (IJPSAT)
ISSN: 2509-0119.

https://ijpsat.org/
Vol. 53 No. 2 November 2025, pp. 396-414

CA: Corrosion allowance (CA=1mm).

The permissible limits are given by the stress formula [9]:

$$S_d = \frac{2}{3} S235JR_y \tag{11}$$

With $S235JR_y$: yield strength ($S235JR_y = 235MPa$).

The choice of design material for our distiller is ordinary steel from a commercially available TPN sheet, 1.5mm thick.

2.2.3 Temperature profile in the distiller

In the case of a cylindrical shell with internal heat sources ($\dot{Q} \neq 0$), heat transfer takes place by steady-state convection in a cylindrical geometry (hollow cylindrical pipe). Let Ri and Re be the inner and outer radius of the cylindrical pipe. The inner and outer walls of the pipe are maintained at variable temperatures Ti and Te respectively.

In cylindrical coordinates, the heat equation is [10]:

$$\alpha_d \left[\frac{\partial^2 T(r,\theta,z,t)}{\partial r^2} + \frac{1}{r}\frac{\partial T(r,\theta,z,t)}{\partial r} + \frac{1}{r^2}\frac{\partial^2 T_{four}(r,\theta,z,t)}{\partial \theta^2} + \frac{\partial^2 T(r,\theta,z,t)}{\partial z^2} \right] + \frac{\dot{Q}}{\rho C_p} = \frac{\partial T(r,\theta,z,t)}{\partial t} \tag{12}$$

Where α_d: thermal diffusivity of the shell ($m^2.s^{-1}$). .

ρ : Shell density ($kg.m^{-3}$).

C_p: Heat density of the shell ($J.kg^{-1}.K^{-1}$).

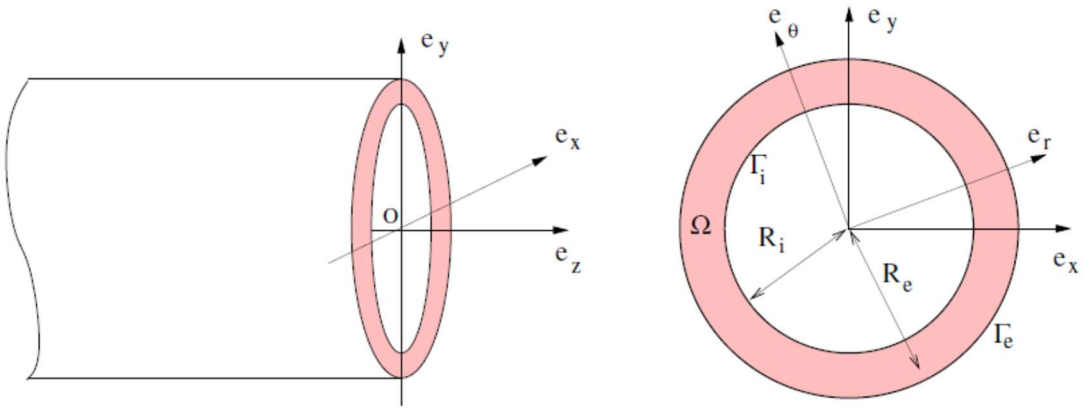

Figure 3: *Heat conduction in a tube*

We're only interested in a plane problem in a section far from the ends of the hollow cylinder. We are therefore looking for the temperature field $T(r,\theta)$ in an area of interest, which is a disk bounded by the circular edges Γ_i and Γ_e (see Fig.3).

International Journal of Progressive Sciences and Technologies (IJPSAT)
ISSN: 2509-0119.

https://ijpsat.org/
Vol. 53 No. 2 November 2025, pp. 396-414

The cylinder is made of a material for which the thermal conductivity coefficient is k. It contains coals heated to a temperature of Ti=35°C. In the following, we'll assume that the heat flows fast enough to impose its temperature permanently on the cylinder's inner surface. There is no external heat input by volume.

It is assumed that the outer surface of the cylinder is subject to a known h_d imposed outflow condition.

For reasons of symmetry, the isotherms are coaxial cylinders, and the temperature is a function only of the radius r, T=f(r). Consequently, the Laplacian of T becomes:

$$\Delta T = \frac{\partial^2 T}{\partial r^2} + \frac{1}{r}\frac{\partial T}{\partial r} = \frac{1}{r}\frac{\partial}{\partial r}\left(r\frac{\partial T}{\partial r}\right) \tag{13}$$

If there is no internal heat release ($\dot{Q} = 0$) and if α_d constant, the heat equation is written:

$$\alpha_d\left(\frac{\partial^2 T}{\partial r^2} + \frac{1}{r}\frac{\partial T}{\partial r}\right) = \frac{\partial T}{\partial t} = 0 \Rightarrow \frac{1}{r}\frac{\partial}{\partial r}\left(r\frac{\partial T}{\partial r}\right) = 0 \tag{14}$$

The exact solution to this differential equation is:

$$T(r) = a\ln r + b \tag{15}$$

The constants a and b are determined from the boundary conditions.

The boundary conditions are:

Temperature imposed at the edge Γ_i

$$T = 0,\ \forall M \in \Gamma_i \text{ with } \Gamma_i = \left\{M(r,\theta), r = R_i; 0 \le \theta \le 2\pi\right\} \tag{16}$$

Heat flux imposed at the edge Γ_e

$$k\overrightarrow{grad}T.\vec{e_r} = h_d,\ \forall M \in \Gamma_e \text{ with } \Gamma_e = \left\{M(r,\theta), r = R_e; 0 \le \theta \le 2\pi\right\} \tag{17}$$

The temperature field is then given by the expression:

$$T(r) = \frac{h_d R_e}{k}\left(\ln r - \ln R_i\right) \tag{18}$$

Where h_d : Heat flux imposed surface (W).

The heat flux is determined by Fourier's law [11]:

$$\phi = -2\pi kH\frac{T_e - T_i}{\ln\frac{R_e}{R_i}} \tag{19}$$

International Journal of Progressive Sciences and Technologies (IJPSAT)
ISSN: 2509-0119.

https://ijpsat.org/
Vol. 53 No. 2 November 2025, pp. 396-414

Where ϕ : Heat flux (W).

k : Thermal conductivity (W.m^{-1}.°C).

H : cylinder height (m).

At thermal equilibrium: $\phi = h_d$ (20)

The approximate solution of the differential equation is obtained by util method of finite element Galerkin [12].

We note $P(r)$ the weighting function in the domain and $\overline{P}(r)$ that used for the boundary conditions, assuming they have the same symmetry properties.

The weak integral formulation is written:

$$\int_{\Omega} k\Delta T(r)P(r)\,dS + \int_{\Gamma_i} T(r)\overline{P}(r)\,dl + \int_{\Gamma_e}\left(k\frac{dT(r)}{dr} - h_d\right)\overline{P}(r)\,dl = 0\ , \qquad \forall P(r), \overline{P}(r) \quad (21)$$

Developing this equation, we obtain:

$$2\pi\int_{R_i}^{R_e} k\frac{d}{dr}\left(r\frac{dT(r)}{dr}\right)P(r)\,dr + 2\pi R_i T(R_i)\overline{P}(R_i) + 2\pi R_e\left(k\frac{dT(R_e)}{dr} - h_d\right)\overline{P}(R_e) = 0\,,\ \forall P(r), \overline{P}(r) \quad (22)$$

After simplification by integrals taking account of symmetries:

$$\int_{R_i}^{R_e} k\frac{d}{dr}\left(r\frac{dT(r)}{dr}\right)P(r)\,dr + R_i T(R_i)\overline{P}(R_i) + R_e\left(k\frac{dT(R_e)}{dr} - h_d\right)\overline{P}(R_e) = 0 \quad (23)$$

After integration by part of the first term of equation 23, we obtain:

$$-\int_{R_i}^{R_e} k\frac{dT}{dr}\frac{dP}{dr}r\,dr + \left[rk\frac{dT(r)}{dr}P(r)\right]_{R_i}^{R_e} + R_i T(R_i)\overline{P}(R_i) + R_e\left(k\frac{dT(R_e)}{dr} - h_d\right)\overline{P}(R_e) = 0 \quad (24)$$

So, the weak integral formulation of the problem becomes:

$$-\int_{R_i}^{R_e} k\frac{dT}{dr}\frac{dP}{dr}r\,dr + R_e k\frac{dT(R_e)}{dr}P(R_e) - R_i k\frac{dT(R_i)}{dr}P(R_i) + R_i T(R_i)\overline{P}(R_i) + R_e\left(k\frac{dT(R_e)}{dr} - h_d\right)\overline{P}(R_e) = 0 \quad (25)$$

After factoring in identical terms, equation 25 becomes:

$$-\int_{R_i}^{R_e} k\frac{dT}{dr}\frac{dP}{dr}r\,dr + R_e k\frac{dT(R_e)}{dr}\left(P(R_e) + \overline{P}(R_e)\right) - R_i k\frac{dT(R_i)}{dr}P(R_i) + R_i T(R_i)\overline{P}(R_i) - R_e h_d\overline{P}(R_e) = 0 \quad (26)$$

By choosing $P(R_e) = -\overline{P}(R_e)$ and $P(R_i) = -\overline{P}(R_i) = 0$ (which amounts to choosing weighting functions satisfying the condition on Γ_i), we obtain the weak formulation:

International Journal of Progressive Sciences and Technologies (IJPSAT)
ISSN: 2509-0119.

https://ijpsat.org/
Vol. 53 No. 2 November 2025, pp. 396-414

$$\int_{R_i}^{R_e} k\frac{dT(r)}{dr}\frac{dP(r)}{dr}rdr - h_d R_e P(R_e) = 0,\ \forall P(r) \quad (27)$$

We wish to obtain approximations of the solution from the weak formulation using Galerkin's method.

In fact, an approximation is made $T(r) = \sum_{i=1}^{N} q_i \varphi_i(r)$ and the basic functions are used as weighting functions $P(r) = \varphi_i(r)$, remembering that these functions must satisfy the condition $P(R_i) = 0$.

The approximate solution is obtained by solving the linear system:

$$[K]\{q\} = \{f\} \quad (28)$$

With: $K_{ij} = \int_{R_i}^{R_e} k\frac{d\varphi_i(r)}{dr}\frac{d\varphi_j(r)}{dr}dS$ and $f_i = h_d R_e \varphi_i(R_e) = 0$,

To find the approximation, simply choose a linear function of the type $\varphi_1(r) = r - R_i$ that satisfies the condition $T(R_i) = 0$. There are therefore a function and a single unknown scalar parameter q1 and the approximation is written:

$$T_1(r) = q_1\varphi_1(r) = q_1(r - R_i) \quad (29)$$

The calculations give:

$$K_{11} = \frac{k}{2}\left(R_e^2 - R_i^2\right) \text{ and } f_1 = h_d R_e (R_e - R_i)$$

The approximate solution is therefore:

$$T_1(r) = \frac{2h_d}{k}\frac{R_e}{R_e + R_i}(r - R_i) \quad (30)$$

2.2.4 Optimization of the reaction yield

The aim is to determine by experiment and simulation the operating conditions that will ensure good production while avoiding a rise in temperature in the distiller. An experimental methodology is applied for this optimization, based on the use of a design of experiments.

These techniques enable us to define experimentally the relationship between each of the responses and the various factors studied. To achieve our objective, we opted for the use of response surface modeling (RSM), based on the factorial design [13].

Choose a mathematical function that relates the response to the factors. We take a limited development of the Taylor series. The derivatives are assumed to be constant, and the expansion takes the form of a polynomial of varying degrees [13]:

$$y = a_0 + \sum a_i x_i + \sum a_{ij} x_i x_j + \ldots + \sum a_{ii} x_i^2 + a_{ij\ldots z} x_i x_j \ldots x_z \quad (31)$$

Where y is the response or quantity of interest. It is measured during the experiment and is obtained with a given precision.

x_i represent the level assigned to factor i by the experimenter to carry out a test. This value is perfectly known.

International Journal of Progressive Sciences and Technologies (IJPSAT)
ISSN: 2509-0119.

https://ijpsat.org/
Vol. 53 No. 2 November 2025, pp. 396-414

x_j represent the level assigned to factor j by the experimenter to carry out a test. This value is perfectly known.

a_0, a_i, a_{ij}, a_{ii} are the coefficients of the mathematical model adopted a priori. They are not known and must be calculated from the experimental results.

The advantage of modeling the response by a polynomial is that we can then calculate all the responses in the field of study without having to carry out experiments.

To this end, 18 experimental tests were carried out on the prototype, the experimental conditions of which are given in Tables 1, 2 and 3.

Table 1: *Operating conditions for the 1st series.*

1st series of tests	Mass of used VL tires (g)	Steam flow rate (mL/min)	Maximum crucible temperature (°C)	Average heating rate (°C/min)	Average test duration (min)
1	63	8,3	105,2	18,5	55
2	120	16,7	114,8	22,3	45
3	122	16,7	127,4	19,6	60
4	180	25	225,5	33,3	52
5	240	25	Thermocouple problem	-	50
6	300	25	261,5	34,7	55

Table 2: *Operating conditions for the 2nd series.*

2nd series of tests	Mass of BT used bicycle tires (g)	Steam flow rate (mL/min)	Maximum crucible temperature (°C)	Average heating rate (°C/min)	Average test duration (min)
1	63	8,3	221,6	35,9	45
2	120	16,7	167,8	30,5	45
3	122	16,7	Thermocouple problem	-	60
4	180	25	198,4	29,2	60
5	240	25	Thermocouple problem	-	70
6	300	25	160,4	22,9	70

International Journal of Progressive Sciences and Technologies (IJPSAT)
ISSN: 2509-0119.

https://ijpsat.org/
Vol. 53 No. 2 November 2025, pp. 396-414

Table 3: *Operating conditions for 3rd series.*

3rd series of tests	Mass of used MT motorcycle tires (g)	Steam flow rate (mL/min)	Maximum crucible temperature (°C)	Average heating rate (°C/min)	Average test duration (min)
1	63	8,3	282,8	48,5	45
2	120	16,7	280,8	54,2	52
3	122	16,7	330,8	55,3	60
4	180	25	243,5	45,7	30
5	240	25	285,6	42,3	40
6	300	25	278,6	41,9	60

The influence of certain operating parameters (used tire mass, steam flow rate, maximum crucible temperature, average heating rate, average test duration) on distiller performance was evaluated.

For this study, we selected the factors that appear to have an effect on our distiller, namely: temperature and average test duration.

Experimental design was carried out to determine the optimum operating conditions for the vapo-thermolysis process.

The estimated coefficients of the model are determined by a system of 6 equations with 6 unknowns:

$$\begin{cases} y_1 = a_0 + a_1 D_1 + a_2 T_1 + a_{12} D_1 T_1 + a_{11} D_1^2 + a_{22} T_1^2 \\ y_2 = a_0 + a_1 D_2 + a_2 T_2 + a_{12} D_2 T_2 + a_{11} D_2^2 + a_{22} T_2^2 \\ y_3 = a_0 + a_1 D_3 + a_2 T_3 + a_{12} D_3 T_3 + a_{11} D_3^2 + a_{22} T_3^2 \\ y_4 = a_0 + a_1 D_4 + a_2 T_4 + a_{12} D_4 T_4 + a_{11} D_4^2 + a_{22} T_4^2 \\ y_5 = a_0 + a_1 D_5 + a_2 T_5 + a_{12} D_5 T_5 + a_{11} D_5^2 + a_{22} T_5^2 \\ y_6 = a_0 + a_1 D_6 + a_2 T_6 + a_{12} D_6 T_6 + a_{11} D_6^2 + a_{22} T_6^2 \end{cases} \quad (32)$$

With $D_1, D_2, D_3, D_4, D_5, D_6$: column vector of average test duration.

$T_1, T_2, T_3, T_4, T_5, T_6$: column vector of maximum crucible temperature.

$D_1T_1, D_2T_2, D_3T_3, D_4T_4, D_5T_5, D_6T_6$: column vector of interactions between duration and temperature.

$D_1^2, D_2^2, D_3^2, D_4^2, D_5^2, D_6^2$: column vector of quadratic effects of mean test duration.

$T_1^2, T_2^2, T_3^2, T_4^2, T_5^2, T_6^2$: column vector of quadratic effects of temperature.

$a_0, a_1, a_2, a_{12}, a_{11}, a_{22}$: coefficients of the 2nd-order model.

The system of equation 32 is written as a matrix:

International Journal of Progressive Sciences and Technologies (IJPSAT)
ISSN: 2509-0119.

https://ijpsat.org/
Vol. 53 No. 2 November 2025, pp. 396-414

$$\begin{pmatrix} 1 & D_1 & T_1 & D_1T_1 & D_1^2 & T_1^2 \\ 1 & D_2 & T_2 & D_2T_2 & D_2^2 & T_2^2 \\ 1 & D_3 & T_3 & D_3T_3 & D_3^2 & T_3^2 \\ 1 & D_4 & T_4 & D_4T_4 & D_4^2 & T_4^2 \\ 1 & D_5 & T_5 & D_5T_5 & D_5^2 & T_5^2 \\ 1 & D_6 & T_6 & D_6T_6 & D_6^2 & T_6^2 \end{pmatrix} \begin{pmatrix} a_0 \\ a_1 \\ a_2 \\ a_{12} \\ a_{11} \\ a_{22} \end{pmatrix} = \begin{pmatrix} y_1 \\ y_2 \\ y_3 \\ y_4 \\ y_5 \\ y_6 \end{pmatrix} \quad (33)$$

Hence the estimated coefficients:

$$\hat{a} = \left(X^{'}X\right)^{-1} X^{'}y \quad (34)$$

With $X^{'}X$: the information matrix.

$\left(X^{'}X\right)^{-1}$: the dispersion matrix.

$X^{'}$: the transpose matrix of X.

y : the response of experiment measure.

The levels assigned for each factor are calculated as follows:

$$D_i = \frac{Duration - \overline{Duration}}{nb_{test}} \quad \forall i \quad (35)$$

With nb_{test} : number test.

$\overline{Duration}$: average test duration.

$$T_i = \frac{Temperature - \overline{Temperature}}{nb_{essai}} \quad \forall i \quad (36)$$

With $\overline{Temperature}$: average test temperature.

The 2nd degree model is written:

$$\hat{y} = a_0 + a_1D + a_2T + a_{12}DT + a_{11}D^2 + a_{22}T^2 \quad (37)$$

This model contains six (6) parameters ($a_0, a_1, a_2, a_{12}, a_{11}, a_{22}$) and a minimum of 18 tests is therefore desirable to properly apply the multiple regression method.

3. RESULTS AND DISCUSSIONS

3.1 Dimensions of the prototype

Table 4 shows the dimensions of the prototype produced.

International Journal of Progressive Sciences and Technologies (IJPSAT)
ISSN: 2509-0119.

https://ijpsat.org/
Vol. 53 No. 2 November 2025, pp. 396-414

Table 4: *Dimensions of the dry distiller*

Dimensions	Crucible	distiller
Volume (L)	0,91	23
Diameter (mm)	90	300
Height (mm)	143	330
Thickness (mm)	3	1,5

The prototype's characteristic dimensions are shown in Fig.3.

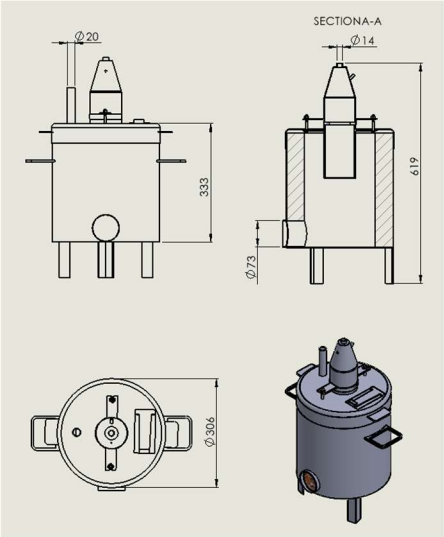

Figure 3: *Drawing of a dry distillation unit [4].*

Photo 1 shows the distillation unit in operation.

Photo 1: *Dry distiller*

The results obtained are not far from the values found in other literature. Table 5 shows the dimensions of the dry distillation unit from [6].

International Journal of Progressive Sciences and Technologies (IJPSAT)
ISSN: 2509-0119.

https://ijpsat.org/
Vol. 53 No. 2 November 2025, pp. 396-414

Table 5*: *Dimensions of the dry distillation unit [6].

Dimensions	Crucible	Distiller
Volume (L)	4	15
Diameter (mm)	125	225
Height (mm)	300	370
Thickness (mm)	2	2

3.2 Actual and approximate temperature profile

The distiller's thermal and geometric data are as follows:

Thermal conductivity of refractory brick: k=0, 84W.m^{-1}°C.

External temperature: Te=25°C.

Internal temperature: Ti = 1220°C.

Internal radius: Ri = 0,10m.

Outer radius: Re = 0,15m.

Height: H=0,33m.

Equation 18 becomes:

$$T(r) = 917(\ln r + 2,3) \tag{38}$$

Figure 4 shows the actual temperature profile.

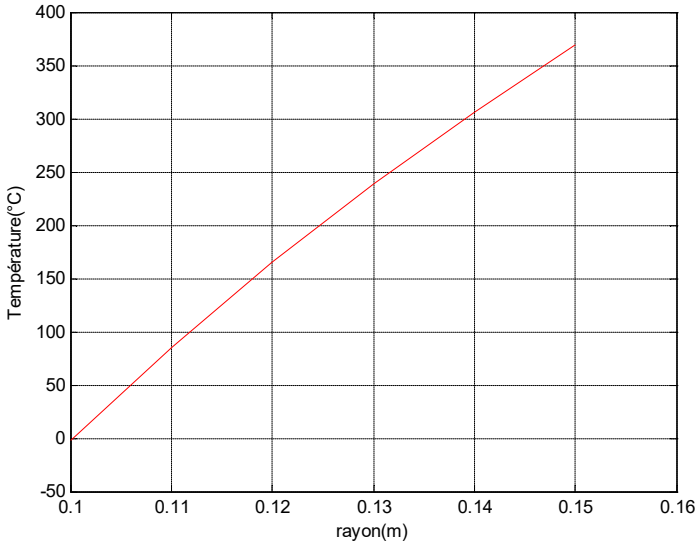

***Figure 4:** Actual temperature profile.*

The temperature variation increases with the geometric radius of the distillation unit. The thickness of the refractory brick acts as thermal insulation for the distillation furnace, and its value lies between 0,10 m and 0,15 m.

International Journal of Progressive Sciences and Technologies (IJPSAT)
ISSN: 2509-0119.

https://ijpsat.org/
Vol. 53 No. 2 November 2025, pp. 396-414

Equation 30 becomes:

$$T_1(r) = 7333(r - 0{,}1) \quad (39)$$

Figure 5 shows the actual and approximate temperature profile.

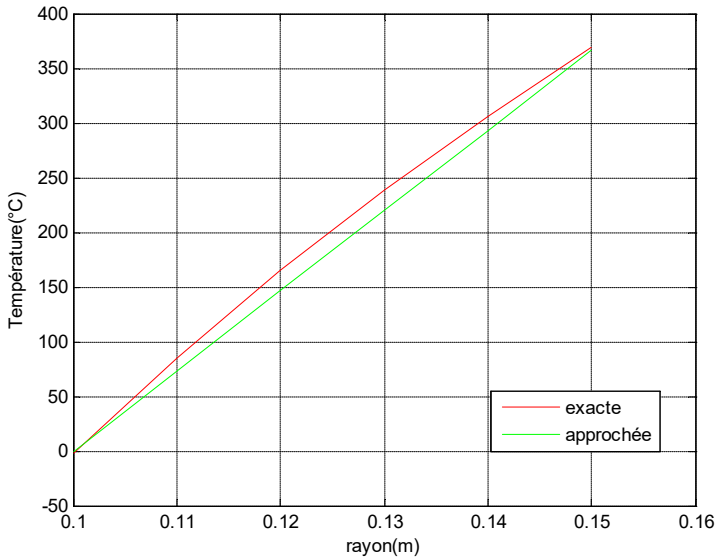

Figure 5: *Actual and approximate temperature profile.*

3.3 Optimum reaction efficiency

3.3.1 Experimental matrices for the three series and their models

Tables 6, 7 and 8 show the experimental matrices for the three series carried out (VL, BT, MT).

Table 6: *Experimental matrices for the 1st series.*

1st series of test	Average test duration (min)	Maximum crucible temperature (°C)	D_i	T_i	Liquid (%.m)	Solid (%.m)	Gas (%.m)
1	55	105,2	0,36	-5,68	37,07	3,02	59,91
2	45	114,8	-1,30	-4,04	38,44	5,76	55,8
3	60	127,4	1,19	-1,94	50,93	5,17	43,9
4	52	225,5	-0,14	14,40	33,56	7,22	59,22
5	50	0	-0,47	-23,18	63,51	9,36	27,13
6	55	261,5	0,36	20,40	72,19	11,41	16,4

$\overline{Duration} = 52{,}83\,\text{min}$.

$\overline{Temperature} = 139{,}07°C$.

International Journal of Progressive Sciences and Technologies (IJPSAT)
ISSN: 2509-0119.

https://ijpsat.org/
Vol. 53 No. 2 November 2025, pp. 396-414

Table 7: *Experimental matrices for 2nd series.*

2nd series of tests	Average test duration (min)	Maximum crucible temperature (°C)	D_i	T_i	Liquid (%.m)	Solid (%.m)	Gas (%.m)
1	45	221,6	-2,22	16,15	31,12	3,80	65,08
2	45	167,8	-2,22	7,18	33,07	6,54	60,39
3	60	0	0,28	-9,72	59,80	6,54	33,66
4	60	198,4	0,28	12,28	86,05	10,63	3,32
5	70	0	1,94	-9,72	71,32	15,41	13,27
6	70	160,4	1,94	5,95	72,68	20,58	6,74

$\overline{Duration} = 58,33\min$.

$\overline{Temperature} = 124,7°C$.

Table 8: *Experimental matrices for 3rd series.*

3rd series of tests	Average test duration (min)	Maximum crucible temperature (°C)	D_i	T_i	Liquid (%.m)	Solid (%.m)	Gas (%.m)
1	45	282,8	-0,47	-0,15	53,17	2,73	44,1
2	52	280,8	0,69	-0,48	57,27	4,68	38,05
3	60	330,8	2,03	7,85	60	4,58	35,42
4	30	243,5	-2,97	-6,69	27,22	7,61	65,17
5	40	285,6	-1,30	0,32	30,93	9,85	59,22
6	60	278,6	2,03	-0,85	62,93	12,78	24,29

$\overline{Duration} = 47,83\min$.

$\overline{Temperature} = 283,68°C$.

The liquid yield models for the three experimental series are as follows:

$$\hat{y}_{L_1} = 39,1 + 14,68D + 0,18T + 3,18DT + 1,45D^2 + 0,001T^2 \quad (40)$$

With estimated mean: $\overline{y_{L_1}} = 39,1\%$

$$\hat{y}_{L_2} = 100,26 + 17,06D + 2,37T - 1,71DT - 12,07D^2 - 0,27T^2 \quad (41)$$

With estimated mean: $\overline{y_{L_2}} = 100,26\%$

International Journal of Progressive Sciences and Technologies (IJPSAT)
ISSN: 2509-0119.

https://ijpsat.org/
Vol. 53 No. 2 November 2025, pp. 396-414

$$\hat{y}_{L_3} = 56,64 + 4,25D - 18,37T - 19,28DT - 13,84D^2 + 8,16T^2 \quad (42)$$

With estimated mean: $\overline{y_{L_3}} = 56,64\%$

The solid yield models for the three experimental series are as follows:

$$\hat{y}_{s_1} = 2,92 + 0,06D + 0,09T + 0,04DT + 1,69D^2 + 0,01T^2 \quad (43)$$

With estimated mean: $\overline{y_{S_1}} = 2,92\%$

$$\hat{y}_{S_2} = 10,19 + 3,61D + 0,25T - 0,006DT + 0,75D^2 - 0,02T^2 \quad (44)$$

With estimated mean: $\overline{y_{S_2}} = 10,19\%$

$$\hat{y}_{s_3} = 2,56 + 1,23D + 5,58T + 5,41DT + 5,72D^2 - 2,5T^2 \quad (45)$$

With estimated mean: $\overline{y_{S_3}} = 2,56\%$

The gas yield models for the three experimental series are as follows:

$$\hat{y}_{G_1} = 57,98 - 14,74D - 0,28T - 3,22DT - 3,14D^2 - 0,01T^2 \quad (46)$$

With estimated mean: $\overline{y_{G_1}} = 57,98\%$

$$\hat{y}_{G_2} = -10,46 - 20,67D - 2,62T + 1,72DT + 11,31D^2 + 0,29T^2 \quad (47)$$

With estimated mean: $\overline{y_{G_2}} = -10,46\%$

$$\hat{y}_{G_3} = 40,80 - 5,48D + 12,79T + 13,87DT + 8,11D^2 - 5,66T^2 \quad (48)$$

With estimated mean: $\overline{y_{G_3}} = 40,80\%$

3.3.2 Validation of numerical and experimental results

Entering the results of the 18 trials into the experimental design, together with the two factors selected as most influential in the process, provided the parameters leading to optimum yields (Table 9).

Table 9: *Optimum yields*

N° series	Average duration of trials (min)	Average crucible temperature (°C)	Liquid (%.m)	Solid (%.m)	Gas (%.m)
1 (VL)	52,83	139,07	39,1	2,92	57,98
2 (BT)	58,33	124,7	100,26	10,19	-10,46
3 (MT)	47,83	283,68	56,64	2,56	40,80

Several experiments carried out under these optimum conditions led to a test duration of around 1 hour and a maximum crucible temperature of 285,6°C.

The experimental results were compared with those deduced by the mathematical model for this type of reaction. Only the yields of the second series (BT) were overestimated in liquid (100.26%m.) compared with the gas obtained (-10.46%m.). This is due to problems with the thermocouple used during the measurements, and confirms that the sum total is always equal to 100%m. Comparing these two results, we find that as the maximum crucible temperature increases and the average duration of the tests decreases (1st and 3rd series), the yields of the liquid increase in relation to those of the gas obtained. These two yields are clearly confirmed in Tables 6, 7 and 8.

4. CONCLUSION

In this article, we set out to dimension and design a dry distillation prototype using the elementary cylinder geometry method. Using this method, we obtained the respective dimensions of the crucible and the main furnace of the distiller.

In the second part, we modeled the distiller's temperature using two solution methods: the exact method for solving a one-dimensional heat equation with its imposed boundary conditions for temperature and heat flux, and the approximate Galerkin finite-element method to obtain the actual and approximate profiles of the radial temperature field. The curves obtained by simulation (Figure 5) are very close.

In the third section, we optimized the yield of the reaction-taking place in the distillation crucible. The method used consisted in determining the operating conditions by experiment and simulation, while ensuring the correct production of pyrolytic products and limiting any rise in temperature in the distillation chamber. Response surface modeling was developed using an eighteen (18)-trial factorial design. Experimental design is established in order to obtain matrix equations solved by the multiple regression method. The model obtained is a 2nd degree linear equation with two (2) influential factors (duration and maximum crucible temperature) and six (6) parameters. The coefficients of this model are estimated from the experimental results. The numerical results of the model obtained (optimum product yield) are in line with the experimental results (Tables 6, 7, 8 and 9).

ACKNOWLEDGMENTS

I would like to thank the technical staff at the precision engineering workshop at the University of Antsiranana (Madagascar) for producing the dry distillation prototype. I would also like to thank the Research Laboratory (CNRIT) for the experimental phase of the vapor thermolysis process for used tires applied to this prototype.

Funding provided by myself.

REFERENCES

[1] ABDERRAZK Z., SLIMANE R., 2013, "*Temperature control in a batch reactor*", Master's thesis, Université Mohamed Khider-Biskra, Algeria, p48.

[2] VILLERMAUX J., 1993, "*Génie de la réaction chimique : conception et fonctionnement des réacteurs*", Génie des procédés de l'Ecole de Nancy, p398, 399.

[3] Sabrina M., 2015, "*Calcul du réacteur fermé adiabatique et chauffe*", Thesis in Process Engineering, Chemical Engineering, Faculty of Science and Technology, Université Mohamed Khider-Biskra, Algeria.

[4] Bird B.B., Stewart W.E., Lightfoot E.N., 2007, "Transport Phenomena", 2nd Edition, John Wiley & Sons. Chapter 7, p.204.

[5] Moulin L., 2018, "*Vapo-thermolysis of used tires. Valorisation du noir de carbone récupéré, relation procédé-produit*", PhD thesis, Ecole Nationale Supérieure des Mines d'Albi-Carmaux, University of Toulouse, France.

[6] « *Formule de géométrie élémentaire* », 2015, Grand Dictionnaire LAROUSSE.

[7] SolidWork, 2021, Technical drawing software.

[8] Henini G., 2019-2020, "*Cours Génie de la reaction 2: Réacteurs Poly-Phasiques*", Faculté de Technologie, Université Hassiba Benbouali de Chelf, Algérie.

[9] Fatima M., 2021, "*Réservoirs de stockage : Méthodologie de calcul et analyse sécuritaire*", 22nd French Mechanical Congress, Lyon-France, August 24-28, 2015.

[10] D. FREDON, L. PORCHERON, 2014 « Le *Formulaire PCSI-PTSI-PC-PSI-PT*», DUNOD.

[11] Jean-Luc B., Andrzej K., Jean-Rodolphe P., 2010, « Cours et exercices à l'Introduction aux transferts thermiques », DUNOD.

[12] Yves D., 2011, "*Méthode des éléments finis : thermique*", Université de Mans, France.

[13] Claude H., 2009, "*Modélisation et Optimisation*", Faculté des Sciences Pharmaceutiques de Tours, France.